Journal of Colloid and Interface Science **236,** 60–66 (2001)
doi:10.1006/jcis.2000.7392, available online at http://www.idealibrary.com on IDEAL®

Dispersion Destabilization in Magnetic Water Treatment

L. C. Lipus,*,[1] J. Krope,† and L. Crepinsek*,[1]

*Faculty of Mechanical Engineering, and †Faculty of Chemistry and Chemical Technology, University of Maribor, Smetanova 17, 2000 Maribor, Slovenia

Received March 7, 2000; accepted December 18, 2000

The destabilization of fine nonmagnetic particles as one of the possible mechanisms for magnetic water treatment (MWT), an alternative method for scale control in industrial water processing and amelioration of dispersion separations, is discussed. Numerical results (based on an electrical double-layer theory) for the theoretical model of surface neutralization due to ion shifts from the bulk of the solution toward the particle surfaces, are presented to show the theoretical possibility of accelerated coagulation of scale-forming particles during and after MWT. © 2001 Academic Press

Key Words: **water treatment; magnetic hydrodynamics; water dispersion systems.**

NOMENCLATURE

a	Particle radius, m
B	Magnetic field density, V s/m^2
c	Molar ion concentration, mol/m^3
c_∞	Molar concentration of electrolytes in the bulk of the solution, mol/m^3
e	Electrical charge, A s
e_0	Electron charge $= 1.6 \times 10^{-19}$ A s
E_m	Magnetic attraction energy, J
E_w	Intermolecular interaction energy, J
E_T	Total interaction energy between particles, J
F	Faraday constant $= 9.6 \times 10^4$ A s mol
$F_{g,b}$	Difference between gravitation and buoyancy force, N
F_L	Lorentz force, N
F_{vis}	Viscosity force, N
g	Gravity constant $= 9.8$ m/s^2
k_B	Boltzmann constant $= 1.38 \times 10^{-23}$ J/K
k_H	Hamaker constant, J
k_m	Auxiliary magnetic parameter, J/m^3
l_{Ti}	Diffusion length of i ion, m
L	Distance between centers of two particles, m
M	Relative molecule mass, dimensionless
n	Number of dispersion passages through MWT device, dimensionless
P	Auxiliary parameter, defined by Eq. [20], dimensionless
Q	Auxiliary parameter, defined by Eq. [21], V
r	Ion radius, m
R	Universal gas constant $= 8.3$ J/mol K
s	Relative distance between particles, L/a, dimensionless
t	Time, s
t_{des}	Ion desorption time from Stern layer, s
t_i	Ion relaxation time in bulk solution, s
T	Absolute temperature, K
v	Flow velocity of dispersion through the channel of MWT device, m/s
W	Characteristic parameter, defined by Eq. [17], dimensionless
x	Radial coordinate, m
Δx	Lorentz shift of ion, m
Z	Ion valence, dimensionless

Greek Symbols

α	Auxiliary parameter, defined by Eq. [5], 1/V
δ	Thickness of Stern layer, m
ε	Water dielectricity, A s/Vm
η	Water viscosity, Ns/m^2
κ	Debye–Hückel parameter, 1/m
ϕ	Radial angle, rad
φ_δ	Electric potential at Stern border before MWT, V
$\varphi_{\delta m}$	Electric potential at Stern border after single MWT, V
$\varphi_{\delta n}$	Electric potential at Stern border after n passages through MWT device, V
μ_0	Vacuum magnetic permeability $= 4\pi \times 10^{-7}$ V s/A m
χ	Magnetic susceptibility, dimensionless
ρ_l	Mass density of water, kg/m^3
ρ_s	Mass density of solid, kg/m^3
σ	Surface charge density, A s/m^2
τ	Retention time of dispersion in channel of MWT device, s

INTRODUCTION

In many industrial processes that use natural water supplies scale formation is a common and costly problem. Magnetic water treatment (MWT) plays an increasing important role among chemical water conditioning methods regarding scale control and amelioration of dispersion separations (1, 2). The first patent

[1] To whom correspondence should be addressed. E-mail: lucija.crepinsek-lipus@uni-mb.si.

0021-9797/01 $35.00

was registered in Belgium by Vermeiren (3) in 1945. As was reported by Hibben for the USA Army, in 1975, strong electromagnets in high-temperature water systems had been used with good economic effects in the former Soviet Union (4). Since then, the American opinion became more amenable to such water treatment (5). Nowadays, many MWT devices of different configurations and capacities are available in the European market, such as Perma-Solvent (Stuttgart), Magneta (Baden Wurtenberg), Wibro (Rahden), Eibl (Nürnberg), SKW (Friederichsdorf), and others.

Despite several decades of practical use and a great need for such environmentally friendly and economic solutions, the efficiency of these devices still remains unclear due to an incomplete understanding of how MWT devices affect treated water.

This mechanism is complex, consisting of the modified crystallization of scale-forming components and modified dispersion stability. These effects cannot be explained by magnetic attraction among dispersed particles because the main scale components (i.e., $CaCO_3$, $CaSO_4 \cdot 2H_2O$, and SiO_2) form fine nonmagnetic particles. Theoretical research of magnetic coagulation was done by Svoboda (6, 7). Numerical results present the possibility of enhanced magnetic coagulation and flocculation of the fine magnetic particles of hematite, while experimentally observed coagulation of the main scale components, which have weak magnetic properties, could not be explained by the mechanism of magnetic interparticle attractions.

The magnetic field density B, demanded for the magnetic coagulation of SiO_2, has been much higher than the practical values of magnetic field density in MWT devices, which efficiently operate in the range from 0.05 to 1 V s/m^2. Other main scale components, $CaCO_3$ and $CaSO_4 \cdot 2H_2O$, have slightly weaker magnetic properties (Table 5) and would give similar results.

Therefore, MWT effects cannot be explained in such a simple way, but an explanation might be found in the changes of ion distributions and ion hydrations in the nearness of dispersed particle surfaces. Regarding this, Krylov *et al.* (8, 9) experimentally confirmed magnetically enhanced coagulation of $CaCO_3$ dispersion. Results pointed out surface neutralization as the cause of the coagulation. The coagulation rate increased by increasing the magnetic field density and the flow velocity of dispersion through the magnetic field, respectively.

THE LORENTZ FORCE EFFECT ON COLLISION PROBABILITY

MWT devices are very different in their constitution. In most industrial MWT devices, water dispersion flows through a perpendicular magnetic field. In some cases, the magnetic field is alternated or pulsed and in the majority the flow is turbulent. For the following analysis, the model of a basic cell (Fig. 1) has been used with working parameters (v, water flow velocity through working channel, B, perpendicular density component of applied magnetic field, and τ, retention time of dispersion in the working channel) in ranges recommended from practical experiences of successful MWT applications. Namely, in most

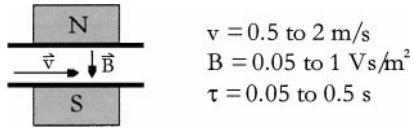

FIG. 1. Scheme of basic cell of MWT device.

MWT experiments, the value of the technical module $B\tau v$ has been shown as the most important parameter for the efficiency of MWT devices.

When the dynamic type of MWT is used, the dispersion flows through the magnetic field, causing Lorentz force F_L, which acts on every electrical charged particle (with electrical charge e) moving (with velocity rate v) through the magnetic field (with density B) as shown in Eq. [1] (10).

$$\mathbf{F}_L = e\mathbf{v} \times \mathbf{B}. \qquad [1]$$

The collision probability of ions in the bulk of solution depends on their thermal movement, precisely, on the average diffusion length l_{Ti} (Fig. 2b).

The Lorentz force could have an influence on that collision probability. For thermal moving ions with velocity $v(t)$, the time average of this velocity (the first term in Eq. [2], (11)) is equal to zero for small time interval t; therefore, the average Lorentz force could be simply expressed by Eq. [1], where ion velocity v is the flow velocity of water and charge e is Ze_0 for ion valence Z.

$$\langle \mathbf{F}_L \rangle = \frac{1}{t}\int \mathbf{F}_L(t)\,dt = \frac{1}{t}\int e[\mathbf{v}(t)+\mathbf{v}]\,dt \times \mathbf{B}$$
$$= \frac{1}{t}\int \mathbf{v}(t)\,dt \times \mathbf{B}\cdot e + \frac{1}{t}\int dt \cdot e\mathbf{v} \times \mathbf{B}. \qquad [2]$$

According to the definition of vector product, the Lorentz force effect on ions in the bulk of the solution could only be

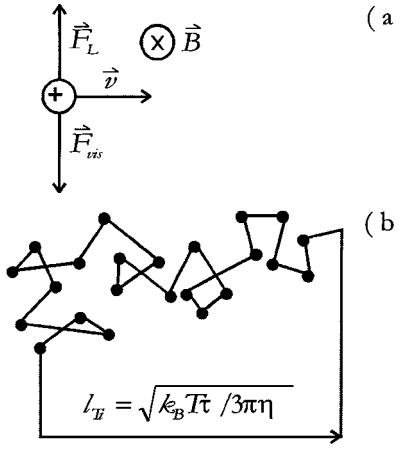

FIG. 2. The ion traveling through the magnetic field and its thermal movement.

TABLE 1
Lorentz Ions Shifts and Relaxation Times at Bv = 0.2 V/m and τ = 0.1 s for Some Ions at Room Temperature

i	Na^+	Mg^{2+}	Ca^{2+}	SO_4^{2-}
r_i (10^{-10} m)	0.95	0.65	0.99	2.3
M_i	23	24	40	96
Δx_i (nm)	1.8	5.3	3.4	1.5
$\Delta x_i / 1_{Ti}$ (10^{-4})	0.8	2.0	1.6	1.1
$\Delta t_i = \Delta x_i (M_i/2RT)^{1/2} (10^{-11}$ s)	0.4	1.2	1.0	0.7

determined by a consideration of product evB, where v is the component of water flow velocity, perpendicular to the magnetic field direction. The ion shift by Lorentz force is retarded by viscosity force F_{vis} (determined by the Stokes equation [3]), as is shown in Fig. 2a. The value of the viscosity force is equal to the Lorentz force in accordance with Newton's law for force balance. In this way, the shift Δx_i is derived as a relationship [4] and will be referred to as the Lorentz shift.

$$F_{vis} = -6\pi\eta r_i \frac{\Delta x_i}{\tau} \quad [3]$$

$$\Delta x_i = \frac{e_0}{6\pi\eta} \frac{z_i}{r_i} (B\tau v). \quad [4]$$

In Table 1, the values of Δx_i and l_{Ti} for some main ions of natural waters are presented. The ratio $\Delta x_i / l_{Ti}$ is practically of order 10^{-4}. Relaxation times Δt_i needed for the reconstructing of the original state of the bulk solution after finishing the treatment are also presented in Table 1 and are practically of order 10^{-11} s. These calculations under working MWT conditions prove that the Lorentz force has very little or no effect on the collision probability of ions in the bulk solution.

On the other hand, the Lorentz effect on collisions among solid particles is significant only at upper values of operational parameters in model Fig. 1. For large particles, the condition [5] is estimated, where the Lorentz force quantifies at least 20% of the difference between the gravitation and buoyancy forces. Analogously, the condition [6] is estimated for small particles, where the ion shift quantifies at least 20% of the diffusion length. The particle radius interval $a = 0.27$ to 1.76 mm could be evaluated at practical values $Bv = 2$ V/m and $t = 0.5$ s from these conditions:

$$\frac{F_L}{F_{gb}} = \frac{\sigma B v 4\pi a^2}{g(\rho_s - \rho_l)4\pi a^3/3} \geq 0.2 \Rightarrow a \leq \frac{15\sigma Bv}{g(\rho_s - \rho_l)}, \quad [5]$$

$$\frac{\Delta x}{l_n} = \frac{2\sigma(B\tau v)a/3\eta}{\sqrt{k_B T \tau/3\tau\eta a}} \geq 0.2 \Rightarrow a \geq \left(\frac{0.1}{\sigma Bv}\right)^2 \left(\frac{k_B T \eta}{\tau}\right)^{1/3}. \quad [6]$$

This narrow interval of relatively large particles approximates rapidly toward 0.5 μm by lowering $(B\tau v)$ and practically disappears when condition [7] is satisfied:

$$(Bv)^5 \tau \leq 0.0555. \quad [7]$$

In a practical example of a 0.2-m-long working channel and 2 m/s flow velocity through a homogenous magnetic field of density 0.26 V s/m^2, the Lorentz concentration effect is negligible.

QUALITATIVE EVALUATION OF THE NEUTRALIZATION

Lorentz ion shifts Δx_i (Eq. [4]) become essential in the nearness of solid surfaces, where they could cause condensation of the Stern layer on account of the Gouy–Chapman layer. According to the calculations of relaxation times (Table 1), the Gouy–Chapman layer will be immediately renewed by the thermal moving of counterions from the bulk solution, while shifted counterions in the Stern layer will remain adsorbed for a longer time according to desorption time estimations for main bivalent ions of natural waters (Table 2). Without strong adsorption and electrostatic attractions, t_0, the time for stepping out from the Stern layer, would be of the order 10^{-11} s, while the values of desorption time t_{des} are longer for Boltzmann's factor. If we exclude the ion adsorption energy, the estimation of minimal desorption time could be reached from the energy of electrostatic ion attraction $Z_1 Z_2 e_0^2 / 4\pi\varepsilon\delta$, where approximations $\delta \approx 5 \times 10^{-10}$ m and $\varepsilon \approx 2.5 \times 10^{-10}$ A s/V m are taken (12).

For spherically dispersed particles (Fig. 3), the action of the Lorentz force would lead to the counterions flowing around the sphere to move downward. This counterions desorption from the Stern layer at the bottom of the particle is expected to be less intensive than its adsorption on the top due to strong attractions in that layer. On the other hand, the lack of neutralization on the bottom should be renewed immediately after the stepping out of the particle from the magnetic field due to thermal moving of the counterions from the bulk solution.

The probability of coions desorption from the top of the particle (due to opposite orientation of Lorentz force) is negligible for the stable adsorbed ions, which have a desorption energy greater than $10k_BT$ and much greater than the work of the Lorentz force $F_L\delta$, as is shown by the estimation in [8],

$$Ze_0 vB\delta / 10k_B T \leq 10^{-8}, \quad [8]$$

TABLE 2
The Estimation of Desorption Times t_{des} for Different Neutralization Degrees

Neutralization degree	$Z_1 Z_2$	$t_{des} \geq t_0 \exp 4Z_1 Z_2$
$7OH^-/Na^+$ (14%)	7	6 s
$8OH^-/Na^+$ (12.5%)	8	5 min
$9OH^-/Na^+$ (11%)	9	5 h
$3OH^-/Ca^{2+}$ (66%)	6	0.3 s
$4OH^-/Ca^{2+}$ (50%)	8	13 min
$5OH^-/Ca^{2+}$ (40%)	10	27 day
$3H^+/SO_4^{2-}$(66%)	6	0.2 s
$4H^+/SO_4^{2-}$(50%)	8	9 min
$5H^+/SO_4^{2-}$(40%)	10	19 day

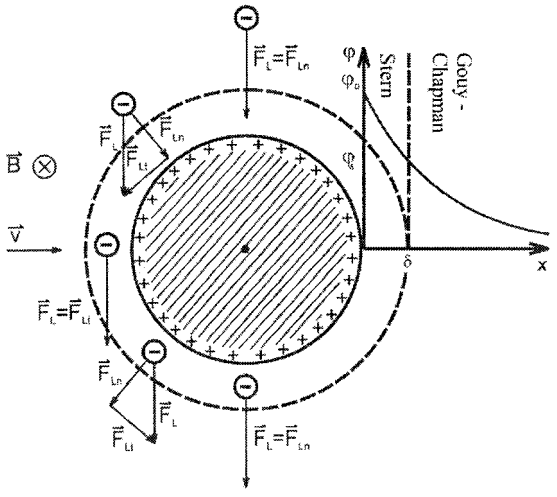

FIG. 3. Scheme of Lorentz counterions flowing around the spherical dispersed particle in the case of positively charged solid surface.

where the parameters are $\delta =$ thickness of Stern layer, $e_0 =$ electron charge, $k_B =$ Boltzmann constant, $T =$ absolute temperature, and $Z =$ ion valence.

An immediate recovery of the Gouy–Chapman layer (in the time of 10^{-11} s), caused by the thermal moving of the counterions from the bulk of the solution, could be presumed. Therefore, in the following calculations, the slope of $\varphi(x)$, electric potential curve, is considered to be practically unchanged during MWT.

QUANTITATIVE EVALUATION OF THE NEUTRALIZATION

A mathematical derivation of the neutralization of dispersed particle surfaces was made on the basis of the electrical double-layer theory ((13) and (14)) for increased counterion concentration in the Stern layer by Lorentz ion shifts Δx (Eq. [11]). The neutralization is expressed by

$$e^{\alpha\varphi'_\delta} - e^{-\alpha\varphi'_\delta} = e^{\alpha\varphi_{\delta+\Delta x}} - e^{-\alpha\varphi_\delta} - \frac{\kappa\Delta x}{2} \qquad [9]$$

$$\alpha = ZF/2RT \qquad [10]$$

$$\Delta x = \Delta x_0 \cos\phi, \qquad [11]$$

where the parameters are $\varphi_\delta =$ electric potential on Stern border ($x = \delta$) before MWT, $\varphi'_\delta = \varphi_\delta$ after finished MWT, $\varphi_{\delta+\Delta x} =$ electric potential on radial distance $x = \delta + \Delta x$, $\phi =$ radial angel, $\Delta x_0 = \Delta x$ on the top of the particle ($\phi = 0$) expressed by Eq. [4], $F =$ Faraday constant, $R =$ universal gas constant, and $\kappa =$ Debye–Hückel parameter.

For mathematical conditions $\kappa\Delta x \le 0.5$ and $\alpha\varphi_\delta \le 0.5$, the relationship of φ'_δ is explicitly expressed by Eq. [12]. After the finished MWT, a tendency for the excess counterions in the Stern layer to distribute uniformly could be expected according to the Stern electrical potential difference at $\phi = 0$ and $\phi = \pi$, and according to the estimation of long desorption times (a few hours lasting 75% and a few days lasting 50%, solid surface neutralization).

The degree of homogenization degree is expected to be higher after treatment with alternating magnets and turbulent flow. However, the homogenization tendency could lead to dipolar fluctuations in the ionic atmosphere, which would result in a heterocoagulation of dispersed particles, expected to be more effective than homocoagulation. A theoretical presumption of complete homogenization with average Stern electrical potential $\varphi_{\delta m}$ (Eq. [13]) was taken to show that even homocoagulation could be of significant.

$$\varphi'_\delta \approx \varphi_\delta - \frac{\kappa\Delta x}{2}\left(\varphi_\delta + \frac{RT}{ZF}\right) \qquad [12]$$

$$\varphi_{\delta m} = \frac{\varphi_\delta}{2} + \int_0^{\pi/2} \varphi'_\delta \frac{\sin\phi}{2}\, d\phi = \varphi_\delta - \frac{\kappa\Delta x}{8}\left(\varphi_\delta + \frac{RT}{ZF}\right) = \varphi_{\delta m}. \qquad [13]$$

According to Eqs. [4] and [13], where e is Ze_0, relative shifts $\kappa\Delta x$, for main ions present in natural waters, are evaluated for the practical case of domestic tap water and represented in Table 3.

Relative shift $\kappa\Delta x$ is a characteristic parameter for the degree of neutralization (Eq. [13]). It is the relative length of the Gouy layer, which is shifted into the Stern layer, because $1/\kappa$ is the first approximation of Gouy layer thickness. At values $\kappa\Delta x \ge 1$, the major part of the counterions would be shifted into the Stern layer. At a higher concentration in the bulk solution, with a higher valence and the lower radius of counterions, a higher neutralization degree is estimated and then a lower operational parameter $B\tau v$ is demanded. Table 4 represents some predictions for the magnetic field density needed for a neutralization degree of 10% at a practical value of working channel length 0.2 m and different solutions.

Results show the strong dependence of treatment efficiency on the composition of the treated water. The effect of treatment with magnetic field density in a practical range from 0.05 to 1 V s/m^2 for highly diluted solutions is negligible. An upper limit of magnetic field density is necessary for medium diluted solutions, and the lower limit satisfies the condition of 10%

TABLE 3

Relative Lorentz Shifts from the Gouy into the Stern Layer in Natural Water with $\kappa^+ = 566/\mu$m for Cations and $\kappa^- = 512/\mu$m for Anions at Operational Module $B\tau v = 0.02$ V s/m

Counterion	r_i/Z_i (10^{-10} m)	Δx_i (nm)	$\kappa\Delta x_i$
Ca^{2+}	0.5	3.4	1.9
Mg^{2+}	0.32	5.3	3.0
Na^+	0.95	1.8	1.0
K^+	1.3	1.3	0.7
Cl^-	1.8	0.9	0.46
NO_3^-	1.9	0.9	0.46
SO_4^{2-}	1.15	1.5	0.77
HCO_3^-	1.85	0.9	0.46

TABLE 4

Magnetic Field Densities for 10% Neutralization of Dispersed Particles with Initially $|\varphi_\delta| = 10$ mV, Treated in a Device with $\tau v = 0.2$ m

c_i (mol/L)	i	κ (1/μm)	$\kappa \Delta x_i$	B (V s/m^2)
10^{-6}	Cl^-	3	0.227	8
10^{-3}	Cl^-	100	0.227	0.25
10^{-3}	SO_4^{2-}	200	0.353	0.12
10^{-2}	Na^+	300	0.227	0.04
10^{-2}	Ca^{2+}	600	0.353	0.02

neutralization degree for common concentrations of natural waters. Such neutralization could last for several hours after finished MWT and could cause coagulation in the natural waters.

ANALYSIS OF COAGULATION FOR MONODISPERSED SPHERICAL PARTICLES

The theoretical possibility of coagulation was analyzed on the basis of the Deryagin, Landau, Verwey, and Overbeck (DLVO) theory (14, 15). The model consists of an equation system [14]–[21] for the interaction energies for monodispersed spherical particles, where E_T is the total interaction energy, E_e is the electric repulsion energy, and E_m is the magnetic attraction energy. The parameter s is the relative distance between the centers of the particles with the same radius a (Fig. 4). The magnetic susceptibility χ and Hamaker constant k_H (a characteristic parameter of intermolecular attraction) are represented in Table 5 for main-scale-forming components. Other parameters are defined in the Nomenclature section.

The principle of this numerical procedure was to observe the extreme points of the $E_T(s)$ curve. To find a coagulation barrier s_{max} and a flocculation basin s_{min}, the Golden Cut method was used. The value of the Stern electrical potential φ_δ was searched to satisfy the coagulation condition [22] for successful particle collision or eventual flocculation at a satisfactory condition [23] and enough small particles distance s_{min}.

$$E_T = E_e + E_W + E_m \quad [14]$$

$$E_W = \frac{-k_H}{6}\left[\frac{2}{s^2-4} + \frac{2}{s^2} + \ln\frac{s^2-4}{s^2}\right] \quad [15]$$

$$s > 50\text{: } E_W = \frac{-16k_H}{9s^6} \quad [16]$$

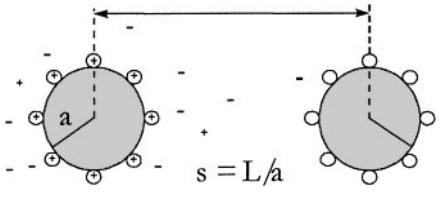

FIG. 4. Dispersed spherical particles.

TABLE 5

Magnetic Susceptibility and Hamaker Constant for Main-Scale-Forming Components (Value of χ for Hematite, Which Is Antiferromagnetic Substance, Is Given at $B = 0.05$ V s/m^2

Solid phase	χ	Ref.	k_H (10^{-20} J)	Ref.
$CaCO_3$	-4×10^{-7}	(16)	1	(17)
$CaSO_4 \cdot 2H_2O$	-3.4×10^{-7} [16]			
SiO_2	-5×10^{-7}	(16)	1	(18)
Hematite Fe_2O_3	2×10^{-2}	(6)	5	(6)

$$E_m = \frac{-k_m a^3}{3}\,\frac{1}{s^3} \quad [17]$$

$$\kappa a < 1\text{: } E_e = \frac{\varepsilon a \varphi_{\delta_m}^2}{s}\,\exp[-\kappa a(s-2)] \quad [18]$$

$$\kappa a > 1\text{: } E_e = \frac{\varepsilon a \varphi_{\delta_m}^2}{2}\,\ln[1+\exp(\kappa a(s-2))] \quad [19]$$

$$k_m = 32\pi^2\chi^2 B^2/3\mu_o \quad [20]$$

$$\kappa = \sqrt{2Z^2F^2c_\infty/\varepsilon RT} \quad [21]$$

$$W = 2\int_2^\infty \exp\left(\frac{E_T}{k_B T}\right)\frac{ds}{s^2} \le 10 \quad [22]$$

$$|E_T(S_{min})| \ge 10k_B T. \quad [23]$$

Typical forms of curves were attained as represented by the example in Fig. 5.

The flocculation possibility was negligible, even for very big particles (i.e., $a = 1\ \mu$m) because of low magnetic susceptibility and the Hamaker constant of $CaCO_3$, $CaSO_4 \cdot 2H_2O$, and SiO_2. When the electrolyte concentration is increased, the estimated flocculation basin tends to be deeper and at closer particles distance s_{min}, but still does not satisfy the flocculation condition [23]. Therefore, only the coagulation of observed scale components could be theoretically predicted.

Furthermore, the value of E_m was negligible in comparison to E_W. Therefore, the conclusion that MWT enhances coagulation by lowering E_e (i.e., φ_δ) could be made.

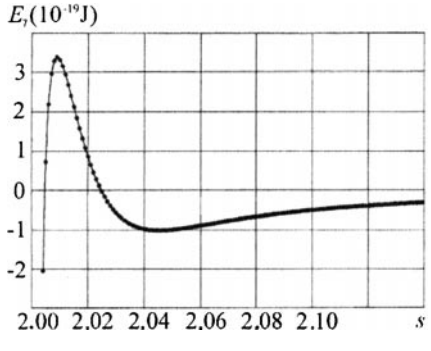

FIG. 5. Coagulation curve at $\kappa = 100/\mu$m, $k_H = 10^{-20}$ J for $a = 1.0\ \mu$m and $\varphi_\delta = 31.6$ mV, which satisfies the condition $W \le 10$.

ENHANCED COAGULATION OF SCALEFORMING PARTICLES BY THEIR NEUTRALIZATION

The theoretical possibility of Lorentz neutralization of dispersed particles in diluted solutions ($\kappa \leq 200/\mu$m and $\varphi_\delta \leq 50$ mV) during MWT was discussed. Here, the model is summarized by Eqs. [4] and [13] for a single flow or by Eqs. [24]–[26] for n passages through the MWT device, where φ_δ is the Stern electric potential before MWT, $\varphi_{\delta m}$ is φ_δ after single MWT, and $\varphi_{\delta n}$ is φ_δ after n passes through the MWT device in the water circulating system. Table 6 represents some values of auxiliary parameters P and Q for chosen examples of diluted counterion solutions.

$$\Delta x = e(B\tau v)/6\pi\eta r \qquad [4]$$

$$\varphi_{\delta m} = \varphi_\delta - \frac{\kappa\Delta x}{8}\left(\varphi_\delta + \frac{RT}{Z_i F}\right) \qquad [13]$$

$$\varphi_{\delta n} = P^n\varphi_\delta - Q\sum_{i=0}^{n-1} P^i \qquad [24]$$

$$P = 1 - \frac{\kappa\Delta x}{8} \qquad [25]$$

$$Q = \frac{\kappa\Delta x RT}{8ZF}. \qquad [26]$$

Figure 6 represents the threshold coagulation curves φ_δ (a) for $CaCO_3$, $CaSO_4 \cdot 2H_2O$, and SiO_2, respectively, in a diluted solution for cases A, B, and C from Table 6. Every water dispersion system with φ_δ, which is lower than the value of the threshold curve, will coagulate. Systems with φ_δ values in areas between curves ($B\tau v$) and (n) are stable before MWT and will coagulate after MWT.

For a hypothetical case of extremely diluted systems (i.e., $\kappa = 3/\mu$m), the introduction of circulating systems is necessary to achieve an essential φ_δ drop. When the values of κ and the counterion valence increase, the required number of passes decreases. By extrapolation of this tendency in natural water systems, where κ is 400 to 600/μm, it could be predicted that only one passage through the MWT device would enable an essential φ_δ drop and enhance the coagulation. Alternatively, the essential coagulation of natural water systems with single MWT could be predicted qualitatively by a comparison of shifts Δx with $1/\kappa$,

TABLE 6
Some Examples of P and Q for Diluted Solutions

Example	A	B	C
κ (1/μm)	3	100	200
Counterions	Cl^-, NO_3^-, HCO_3^-	Cl^-, NO_3^-, HCO_3^-	SO_4^{2-}
B (V s/m^2)	1	0.4	0.1
$\kappa\Delta x$	0.0282	0.37	0.3
P	0.996475	0.995375	0.96250
Q (mV)	0.089296	1.171618	0.474981

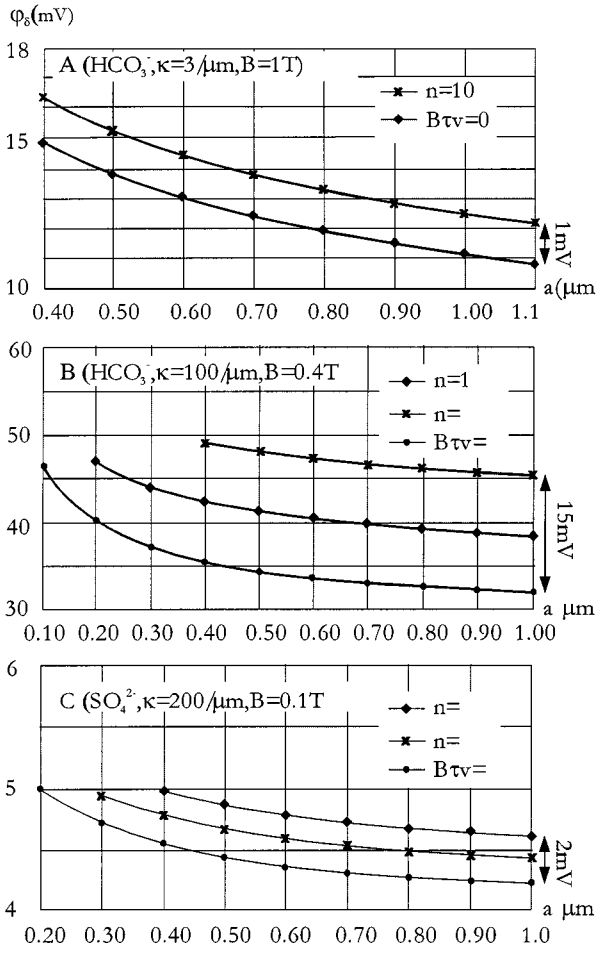

FIG. 6. Threshold coagulation curves for particles with $k_H = 10^{-20}$ J before MWT ($B\tau v = 0$) and after n passes through MWT for cases A, B, and C from Table 4.

the thickness of the Gouy–Chapman layer. For $\kappa \approx 500/\mu$m, the thickness is $1/\kappa = 2$ nm, which is comparable to the practical values of Δx. The shifting of the majority of counterions from the Gouy–Chapman layer into the Stern layer would enable a high degree of particle neutralization and their coagulation.

CONCLUSION

The key to MWT effectiveness for hard scale prevention seems to be the forming of modified large crystals, which in supersaturation conditions serve as a basis for scale precipitation in suspended form. The mechanism of these modifications is considered as complex and strongly linked with the presence of solid surfaces, consisting of several phenomena. Modified hydration could essentially affect water dispersions and solutions even under static magnetic treatment. However, the most successful MWT devices are of dynamic type, with the flowing of supplied water through static or pulsated magnetic field, where the Lorentz effects on solid surfaces could become noticeable and prevail under hydration effects. Preliminary calculations have shown that the concentration effect of the Lorentz force on

dispersed particles is practically negligible for the simple configuration of MWT devices. In such cases, the destabilization effect on water dispersions during and after treatment could only be explained by the neutralization of the dispersed phase surfaces. These could occur due to Lorentz counterion ion shifts from the Gouy–Chapman into the Stern layer, which have relaxation times comparable to the practical times of the magnetic memory.

For example, the affected charge on the surface of the solid phase could result in an asymmetric distribution, which does not immediately relax, when the particles leave the magnetic field and could lead to heterocoagulation.

Alternatively, the partial homogenization of the Stern layer after the finished MWT is also expected to enhance the aggregation of the solid phase by homocoagulation. Relative shift $\kappa \Delta x$ is a characteristic parameter for the neutralization degree. The operational module $B\tau v$ determines the size of Δx. For the accelerated coagulation of dispersed particles in natural waters at a fixed τv length of the working channel, increasing the magnetic field density B is recommended until it becomes $\kappa \Delta x \approx 1$, where the majority of counterions are shifted from the Gouy layer into the Stern layer, while the majority of coions still remain in the bulk of the solution. For greater efficiency, the raising of treatment time τ by the introduction of a circulation system is favorable.

REFERENCES

1. Donaldson, J. D., *in* "HDL Symposia at the Universities of York and Aston, January 1988," *New Scientist*, 117 (1988).
2. Klassen, V. I., *Develop Miner. Proces. Part B Miner. Proces*. 1077–1097 (1981).
3. Vermeiren, T., *Corrosion Technol*. **5,** 215 (1958).
4. Hibben, S. G., "Magnetic Treatment of Water," National Technical Information Service, No. 1622–4, 1973.
5. Grutsch, J. F., USA/USSR Symposium on Physical-Mechanical Treatment of Wastewaters, p. 44. EPA, Cincinnati, OH, 1977.
6. Svoboda, J., *Int. J. Miner. Process.* (8), 377–390 (1981).
7. Svoboda, J., *J. Colloid Interface Sci*. **94** (1) (1983).
8. Krylov, O. T., Rozno, N. A., Funberg, E. I., and Klassen, V. I., *Elektron. Obrabotka Mater*. (2) 53–56 (1987). [UDC 621.332.43:622.693.4]
9. Krylov, O. T., Vikulova, I. K., Eletskii, V. V., Rozno, N. A., and Klassen, V. I., "Influence of Magnetic Treatment on the Electrokinetic Potential of a Suspension of $CaCO_3$," UDC 541.182.65:537.6. Plenum, New York, 1986.
10. Purcell, E. M., "Electricity and Magnetism." Berkeley Physics Course, Vol. 2. McGraw Hill, New York, 1965.
11. Sears, F. W., "An Introduction to Thermodynamics." Addison-Wesley, Reading, MA, 1953.
12. Kitahara, A., and Watenabe, A., "Electrical Phenomena at Interfaces." Dekker, New York, 1984.
13. Voyutski, S., "Colloid Chemistry." MIR Publisher, Moscow, 1978.
14. Hunter, R. J., "Introduction to Modern Colloid Science." Oxford Science Publications, New York, 1996.
15. Verwey, E. J. W., and Overbeck J. Th. G., "Theory of the Stability of Lyophobic Colloids." Elsevier, Amsterdam, 1948.
16. Tebenihin, E. F., Gusev, B. T., "Obrabotka vodi magninim polem v teploenergetike." Moskva, p. 17, Emergija 1970. [UDC 628.163:538.12]
17. Lyklema, J., "Fundamentals of Interface and Colloid Science," Vol. 1. Academic Press, London, 1993.
18. Somasundaran, P., "Fine Particle Processing Conference—Proceedings, Chap. 48, p. 947, Las Vegas, Nevada, 1980.